

Accurate Gain Measurement Technique for Limited Antenna Separations

A. J. van den Biggelaar¹, S. J. Geluk, B. F. Jamroz, D. F. Williams², *Life Fellow, IEEE*,
 A. B. Smolders¹, *Senior Member, IEEE*, U. Johannsen¹, *Member, IEEE*,
 and L. A. Bronckers¹, *Member, IEEE*

Abstract—The Friis equation is often used to determine the gain of antennas but assumes that far-field (FF) conditions are met. For limited antenna separations on the order of the Fraunhofer distance, its use requires a precise estimate of the amplitude centers of the antennas. Using a new antenna gain measurement technique, it is shown that the amplitude center can be very well estimated and that the measurement results can be used to confirm that FF conditions are met. Moreover, reflections caused by scatterers are averaged since multiple measurements are performed. The presented method is particularly useful for anechoic chambers that are limited in size, such as small anechoic chambers for the characterization of, for instance, 5G millimeter-wave phased arrays.

Index Terms—Antenna measurements, gain measurement, measurement errors.

I. INTRODUCTION

ONE of the most important parameters of an antenna is its gain. In the last decades, several measurement techniques were developed to accurately determine the gain of an antenna, such as the state-of-the-art extrapolation measurement technique [1]. Less rigorous measurement techniques often use the Friis equation to determine the antenna gain [2], [3]. By using the Friis equation, some assumptions are made that cannot be satisfied in any practical measurement setup. First of all, the receive antenna is assumed to be excited by a plane wave. In every practical setup, however, the distance between the transmit and receive antennas is finite. Due to the spherical nature of the radiated waves, the limited separation between the two antennas results in a nonuniform phase distribution over the area of the receive antenna. Second, the distance between the antennas has to be known. An antenna has a certain size, which makes it sometimes unclear what should be regarded as the antenna's reference point. In turn, this generates an uncertainty in the distance between the antennas. Lastly, a free-space environment without any scattering is assumed. In every measurement setup, however, reflections are

inevitable, creating multipath components or standing waves between the antennas, potentially disturbing the measurement.

In practice, it is often presumed that the first two assumptions are met when the antennas are separated by the commonly known Fraunhofer distance [4]. In [5], it is shown that if a maximum error as low as 0.05 dB is desired, without applying a proximity correction, the aperture-to-aperture distance between the assessed standard gain horns (SGHs) should be as large as 16 times the Fraunhofer distance. However, in [6], it is shown that if, instead of using the aperture-to-aperture distance, the phase centers are chosen as the reference points of the antennas, the proximity correction is reduced to 0.02 dB if the antennas are separated by the Fraunhofer distance. In [7]–[11], more experimental results are shown, indicating that accurate results can be obtained at one or two times the Fraunhofer distance when using the phase centers as reference points. In these papers, different approaches are taken in order to determine the phase centers. In [6] and [7], a separate measurement requiring a different setup is used to determine the phase centers, whereas in [8]–[10], the phase centers are based on simulations. In [11], an explanation of how the phase centers are determined is omitted.

In this article, a new measurement technique is presented that allows for accurate gain measurements for limited antenna separations. This far-field (FF) technique requires the measurements to be performed for multiple separations between the antennas. The method relies on relative distances (i.e., changes in distance), instead of knowing the exact absolute distance between the antennas. Using this method, the amplitude center of the antennas can be found. This reduces the error in the estimation of the distance between the antennas, subsequently reducing the error in determined gain. Moreover, the method can be used to confirm whether the nonuniform phase distribution over the receiver's aperture is insignificant, and thus whether FF conditions are met. Furthermore, reflections caused by scatterers are (partly) averaged since multiple measurements are performed. Using three K_a -band aperture antennas, measurement data have been acquired and the gain of the three antennas has been determined. We show that, without relying on simulated data or having to perform a separate measurement, the gain of the antennas can be determined accurately for separations of one to two times the Fraunhofer FF distance.

The outline of this article is as follows. In Section II, a discussion on the definition of the phase center and amplitude

Manuscript received November 5, 2020; revised January 29, 2021; accepted February 13, 2021. Date of publication April 5, 2021; date of current version October 6, 2021. (Corresponding author: A. J. van den Biggelaar.)

A. J. van den Biggelaar, S. J. Geluk, A. B. Smolders, U. Johannsen, and L. A. Bronckers are with the Electromagnetics Group, Eindhoven University of Technology, 5600 MB Eindhoven, The Netherlands (e-mail: a.j.v.d.biggelaar@tue.nl).

B. F. Jamroz and D. F. Williams are with the National Institute of Standards and Technology, Boulder, CO 80305 USA.

Color versions of one or more figures in this article are available at <https://doi.org/10.1109/TAP.2021.3069583>.

Digital Object Identifier 10.1109/TAP.2021.3069583

center is given. Section III is devoted to the presented gain measurement technique. In Section IV, measurement results are shown and a model is presented to interpret the obtained results. In Section V, the performance of the technique is evaluated and compared to the extrapolation measurement technique. Finally, in Section VI, conclusions are presented.

II. PHASE AND AMPLITUDE CENTER

In [6]–[11], the phase center is used as the antenna’s reference point. The definition of the phase center is as follows [12]:

The location of a point associated with an antenna such that if it is taken as the center of a sphere the radius of which extends into the FF, the phase of a given field component over the surface of the radiation sphere is essentially constant, at least over that portion of the surface where the radiation is significant.

This definition is ambiguous, as the resulting location depends on which portion of the radiation sphere is assessed. For instance, it is shown in [6] that depending on the choice of angular region ($1^\circ \leq \theta \leq 10^\circ$) and principal cut, the location of the phase center of an SGH can vary up to four wavelengths. In addition, to determine the phase center, a separate measurement [6], [7] or simulation [8]–[10] is required, which is generally undesired.

Instead of using the phase center, the amplitude center can also be used as the reference point of the antenna. In [13], the amplitude center is defined as follows:

A point from which the field amplitude varies relatively closely to the inverse distance variation in a specified direction over some distance range.

The concepts of the phase and amplitude center are related as they both describe a point where the radiation seemingly originates from. Based on the definition, however, for a given direction, the amplitude center can be uniquely determined when the separation of the two antennas is “large enough” such that FF conditions are met. This essentially means that the phase variation of the nonuniform phase distribution over the aperture of the receiver has to be insignificant. In turn, this implies that the distance is “large enough” and that FF conditions are met when making the phase distribution over the aperture more uniform by increasing the antenna separation does not alter the calculated gain of the antenna. Moreover, the definition of the amplitude center relies only on radiation from a specified direction. Therefore, finding the amplitude center does not require knowledge (either simulated or measured) of the radiation pattern in another direction than the direction of interest, as is the case for finding the phase center. Due to these advantages, the amplitude center as described in [13] is adopted as the antenna’s reference point in this article for determining the antenna gain.

III. ANTENNA GAIN MEASUREMENT TECHNIQUE

The presented gain measurement technique is based on the Friis equation and is a variation of the three-antenna method [3]. In Fig. 1, a schematic of a typical gain measurement setup for the three-antenna method is shown.

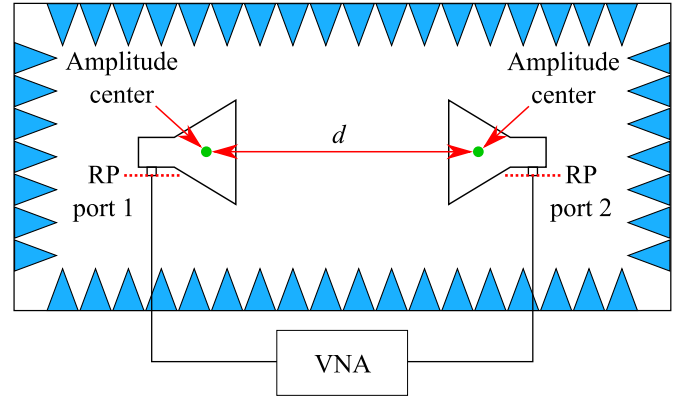


Fig. 1. Schematic of a typical gain measurement setup, including the definition of the RP of each port. The amplitude centers are indicated by the green dots, and the distance d between the antennas is defined from amplitude center to amplitude center.

Two unknown antennas are positioned opposite to each other and are placed in an anechoic chamber. Both antennas are connected to a calibrated vector network analyzer (VNA) such that the reference planes (RPs) are located at the input ports of the antennas. Then, the Friis equation can be cast in the following form:

$$\frac{P_r}{P_t} = |S_{21}|^2 = G_r G_t \left(\frac{\lambda_0}{4\pi d} \right)^2. \quad (1)$$

Here, P_r and P_t are the power levels at the ports of the receiving and transmitting antenna, respectively, and S_{21} represents the measured forward S -parameter. The wavelength in free-space is denoted by λ_0 , d is the distance between the amplitude centers of the two antennas, and G_r and G_t represent the realized gains of the receiving and transmitting antenna, respectively. By performing one single measurement for one given distance, (1) can be used to solve for the product of both realized gains (often referred to as realized pair gain). By performing three measurements, one for each pair of three (unknown) antennas, the realized pair gain of each antenna pair can be determined.¹ Subsequently, the realized gain of each antenna under test (AUT) can be calculated.

Typically, the amplitude center of the antennas is not exactly known. In a conventional three-antenna-method measurement, this leads to an increased uncertainty in d . However, if multiple measurements are performed, while one of the antennas is translated, this uncertainty in d can be reduced. This is done by relying on the relative distances (i.e., changes in distance) between the positions of the antenna that is translated instead of on the absolute distance between the antennas. To show this, the distance between the antennas is from this point onward denoted by $d = d_0 + \Delta d$. Here, d_0 is the unknown distance between the amplitude centers of the antennas of the first measurement. The term Δd represents the relative distance of the translated antenna and can be treated as a measurable (known) variable. By writing $d = d_0 + \Delta d$, (1)

¹In (1), it is assumed that both antennas are linearly polarized and that the polarizations are matched. If the orientation of the polarization of the antennas is unknown and/or one of the three antennas is elliptically polarized, up to six measurements have to be performed to fully characterize the gain of the antennas [1].

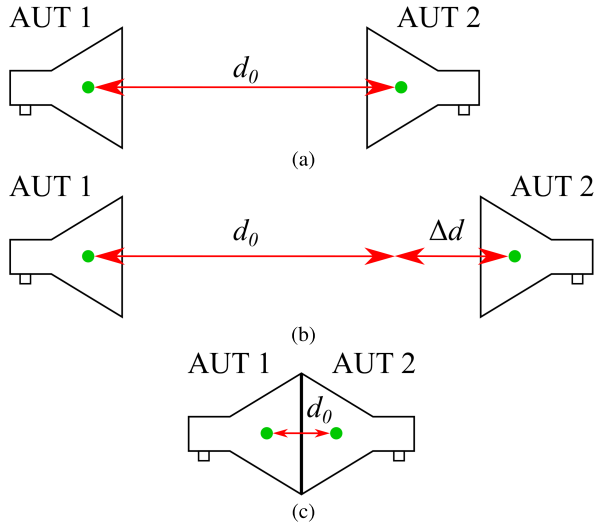


Fig. 2. Schematic of the workflow of a relative-distance sweep measurement, including the definition of d_0 and Δd . (a) Parameter d_0 equals the distance between amplitude centers of the first measurement. (b) In the subsequent measurements, AUT 2 is translated. The value for d_0 is still unknown and is equal to d_0 in the first measurement. It is assumed that the translation Δd can be accurately measured. (c) In the measurement sweeps performed for this article, the aperture planes coincided at the first measurement. This means that in this article, d_0 equals the sum of the amplitude centers of the AUTs with respect to their apertures.

can be written as

$$G_r G_t = \left(|S_{21}| (d_0 + \Delta d) \right)^2 \left(\frac{4\pi}{\lambda_0} \right)^2. \quad (2)$$

The realized gain of an antenna is an FF parameter and is thus per definition independent of d . This means that if FF conditions are met, both sides of (2) are constant. By performing multiple measurements with different antenna separations, both d_0 and the realized pair gain can be determined.

In Fig. 2, the workflow of a relative-distance sweep and a physical interpretation of the parameter d_0 and variable Δd is depicted. Fig. 2(a) represents the first measurement of the relative-distance sweep, indicating the meaning of d_0 . Subsequently, as shown in Fig. 2(b), AUT 2 is translated by some measurable distance Δd and the second measurement is performed. This process continues until sufficient measurements are performed. In Section V, the meaning of sufficient in the context of the presented gain measurement technique is discussed.

In the measurement sweeps performed for this article, the aperture planes of the antennas always coincided at the first measurement. Needless to say, FF conditions are not achieved when the apertures are in such close proximity and the Friis equation is not valid in that case. Having the aperture planes to coincide at the first measurement, however, helps to show the principle of the measurement technique and is not a requisite for utilizing the presented technique. Additionally, having the apertures in contact with each other at the first measurement means that, in this article, d_0 equals the sum of the amplitude centers of the AUTs with respect to their apertures, as illustrated in Fig. 2(c).

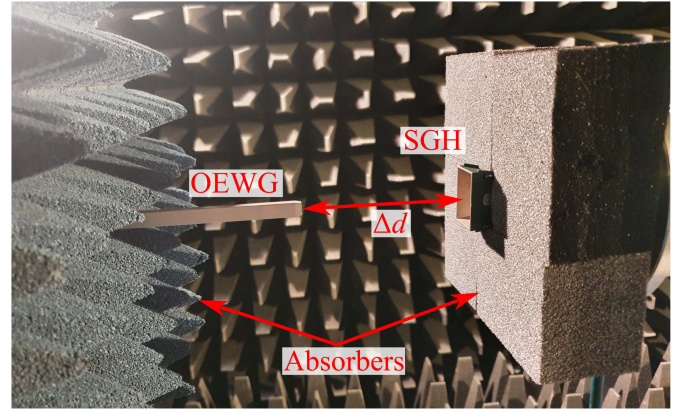


Fig. 3. Measurement setup with the Ka-band OEWG and SGH. The distance sweep started when the aperture planes of the OEWG and SGH coincided, hence, Δd equals in this measurement the aperture-to-aperture distance.

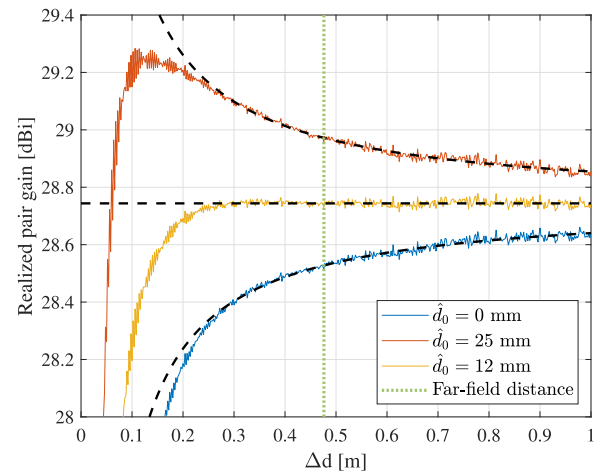


Fig. 4. Determined realized pair gain of an OEWG and an SGH for different estimations of \hat{d}_0 , $f = 40$ GHz. The black dashed lines are calculated using the isotropic radiator model presented in Section IV-B.

IV. MEASUREMENT RESULTS

A. Relative-Distance Sweep: Open-Ended Waveguide (OEWG) and SGH

To illustrate how d_0 can be determined, a measurement using a relative-distance sweep has been performed. In this measurement, an OEWG and SGH operating at Ka-band were positioned opposite to each other (see Fig. 3). The distance between the apertures was linearly increased from 0 to 1 m, in steps of 2 mm, using a motorized linear translation stage.² As a postprocessing step, the realized pair gain has been calculated using (2) for different estimations of d_0 , denoted by \hat{d}_0 , and the results at 40 GHz are shown in Fig. 4.

The realized pair gain calculated using $\hat{d}_0 = 0$ is shown in blue in Fig. 4. Choosing $\hat{d}_0 = 0$ means that in this measurement, the amplitude center of the antennas is estimated to be at the aperture. This implies that for this estimation of \hat{d}_0 , the distance between the antennas is measured from aperture to aperture. It is evident to see that the determined realized pair gain shows an increasing trend with respect to an

²The large amount of 501 measurement points and the small step size of 2 mm is taken to show the principle of the measurement technique and is not required by the technique (see Section V).

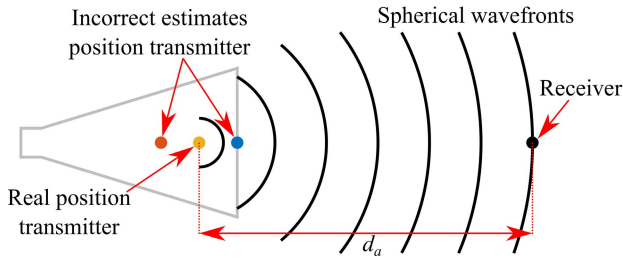


Fig. 5. Schematic of a mathematical model where the antennas are treated as a point object with an isotropic radiation pattern, transmitting perfect spherical wavefronts. The position of the transmitter (yellow) is generally not exactly known, so the distance can be underestimated (blue) or overestimated (red).

increase in separation. This implies that either the nonuniform phase distribution is still significant, the choice of \hat{d}_0 is poor, or a combination of both. In red, the calculated realized pair gain is shown for $\hat{d}_0 = 25$ mm, which is a third of the flare length of the SGH. If the amplitude center of the OEWG is assumed to be at its aperture, this choice of \hat{d}_0 corresponds to estimating the amplitude center of the SGH to be 25 mm inside of the SGH. The red line shows a trend of decreasing pair gain for increasing Δd , preventing an exact determination of the realized pair gain.

In yellow, the resulting pair gain is shown where \hat{d}_0 was determined by a linear least-squares fitting routine. Since the pair gain is by definition independent of separation, this routine determines the value for \hat{d}_0 such that the difference between $|S_{21}|(\hat{d}_0 + \Delta d)$ and a constant is minimized. In other words, \hat{d}_0 is chosen such that it minimizes the residual of the fit of $|S_{21}|(\hat{d}_0 + \Delta d)$ to a constant. For small antenna separations, the nonuniform phase distribution is significant. Hence, in this fitting routine, only data have been used where Δd (i.e., the aperture-to-aperture distance) exceeded the Fraunhofer distance, which is 0.48 m and is indicated by the green dotted line. The parameter \hat{d}_0 was determined to be 12 mm, and it can be seen in Fig. 4 that the calculated pair gain does not show an increasing or decreasing trend for separations larger than the Fraunhofer distance. In fact, already from a separation of 0.3 m, FF conditions appear to be met. The deviations present in the measurement data are most likely due to scatterers in the anechoic chamber and small errors in the exact translation Δd .

B. Isotropic Radiator Model

To better interpret the results obtained for $\hat{d}_0 = 0$ mm and $\hat{d}_0 = 25$ mm in Fig. 4, a mathematical model is constructed where the antennas are treated as isotropic radiators. In Fig. 5, a schematic of the model is depicted. Perfect spherical waves that obey the inverse-square law are originating from the transmitter, which is indicated by the yellow dot. The receiver, indicated by a black dot, is positioned a distance d_a away from the transmitter. Since the receiver is treated as a point object, no phase curvature is present along the receiving aperture. This means that the transfer from one point object to the other can be written as follows:

$$|S_{21}|^2 = \frac{A_{\text{iso}}}{4\pi d_a^2} = \left(\frac{\lambda_0}{4\pi d_a}\right)^2 \quad (3)$$

where A_{iso} is the effective aperture of an isotropic radiator [2]. Suppose that we want to determine the pair gain of the

isotropic radiators using (1), but the distance is not exactly known and an estimate of d_a has to be made. This estimate is denoted by $\hat{d}_a = d_a + \delta d$, with δd being the error in the estimate. By inserting (3) and the estimate \hat{d}_a in (1), the following equation can be derived:

$$\begin{aligned} \hat{G}_r \hat{G}_t &= \left(\frac{\lambda_0}{4\pi d_a}\right)^2 (d_a + \delta d)^2 \left(\frac{4\pi}{\lambda_0}\right)^2 \\ &= \left(\frac{d_a + \delta d}{d_a}\right)^2 \\ &= \left(1 + \frac{\delta d}{d_a}\right)^2 \end{aligned} \quad (4)$$

where $\hat{G}_r \hat{G}_t$ is the estimated realized pair gain for the distance estimation \hat{d}_a .

With this mathematical model in place, let us observe what happens for different estimations of the exact value for d_a . If the distance is correctly estimated, that is, $\delta d = 0$, the resulting pair gain will be independent of antenna separation and the pair gain of the isotropic radiators will be equal to unity, as expected. If, however, the real distance is larger than the estimated distance ($\delta d < 0$), it can be seen in (4) that the estimated realized pair gain is smaller than 1. In contrast, if the real distance is smaller than the estimated distance ($\delta d > 0$), the estimated realized pair gain is larger than 1. Moreover, regardless of sign, for a fixed δd and increasing d_a , the estimated pair gain eventually converges to unity.

This model is analogous to not knowing the amplitude center of a physical antenna and, therefore, underestimating or overestimating the distance between the antennas. Every colored solid line in Fig. 4 is accompanied by a dashed black line. These black lines are constructed using this mathematical model. Hence, they represent the gain of antennas that, independent of separation, can be treated as point objects, for different errors in the estimation of the absolute distance between these point objects. These errors are -12 , 13 , and 0 mm and correspond to the differences in \hat{d}_0 with respect to the estimation found by the least-squares fitting routine. The similar trend observed in the model and the measured data from a separation of about 0.3 m indicates that the increase and decrease in determined realized pair gain shown by the blue and red line, respectively, follow the inverse-square law and thus the antennas can be treated as point objects. This implies that, for separations larger than 0.3 m, the blue and red lines in Fig. 4 are dependent on antenna separation because of a poor choice of reference points and not due to the nonuniform phase distribution over the aperture of the receiving antenna.

Note that the black dashed lines in Fig. 4 converge to the same pair gain for increasing separation. This indicates that the blue and red line also converges to the same pair gain, essentially making the pair gain independent of the choice of \hat{d}_0 for a large value of Δd . This observation is compatible with the statement that if the separation between the antennas is taken to be large enough, the choice of reference point becomes insignificant [6], [14]. However, especially with the increased use of small anechoic chambers for the characterization of, for instance, 5G millimeter-wave phased arrays, separating

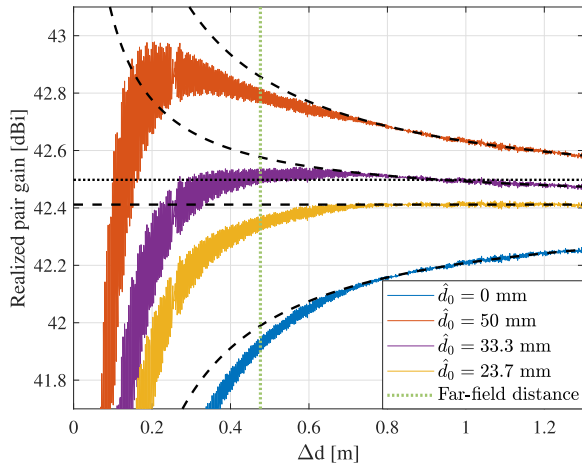


Fig. 6. Determined realized pair gain of two SGHs for different estimations of \hat{d}_0 , $f = 40$ GHz. The blacked dashed lines are calculated using the isotropic radiator model presented in Section IV-B. The black dotted line is meant as visual reference.

the antennas by very large distances is impossible [15], [16]. As can be observed in Fig. 4, for limited separations on the order of the Fraunhofer distance, a poor choice of absolute distance can lead to an error on the order of 0.2 dB in the realized pair gain. This emphasizes the importance of choosing a proper reference point when antennas are measured in anechoic chambers where separations on the order of the Fraunhofer distance can only be achieved and FF conditions are required.

C. Relative-Distance Sweep: SGH and SGH

A similar sweep as described in Section IV-A is performed with two SGHs. In this measurement, the sweep was from 0 to 1.3 m, in steps of 1 mm.³ The pair gain was determined for different choices of \hat{d}_0 and the results are shown in Fig. 6. The values of \hat{d}_0 are selected in the same way as described in Section IV-A. The distance between the antennas is measured from aperture to aperture for $\hat{d}_0 = 0$ mm. For $\hat{d}_0 = 50$ mm, the amplitude center is taken to be 25 mm inside both the SGHs, which equals a third of the SGH's flare length. It can be seen that for these two choices of \hat{d}_0 , the pair gain depends on Δd , indicating a poor choice of \hat{d}_0 . Based on the least-squares fitting routine introduced in Section IV-A, a \hat{d}_0 of 33.3 mm is determined at first. Since FF conditions were met from $\Delta d = 0.3$ m onward for the measurement with the OEWG and SGH shown in Fig. 4, initially, data were used in the fit to estimate d_0 of the measurement with two SGHs that exceeded $\Delta d = 0.3$ m. The resulting pair gain is shown in Fig. 6 in purple. It is evident to see that the pair gain is not constant with respect to separation. In fact, a regular pattern in the trend can be identified. Around $\Delta d = 0.3$ m, the realized pair gain is below 42.5 dBi, as indicated by the black dotted line. From about $\Delta d = 0.4$ m to $\Delta d = 0.9$ m, the pair gain exceeds 42.5 dBi, and from $\Delta d = 0.9$ m it drops again below 42.5 dBi. This regular pattern being present indicates that FF conditions are not yet met from $\Delta d = 0.3$ m.

³The large amount of 1301 measurement points and the small step size of 1 mm is taken to show the principle of the measurement technique and is not required by the technique (see Section V.)

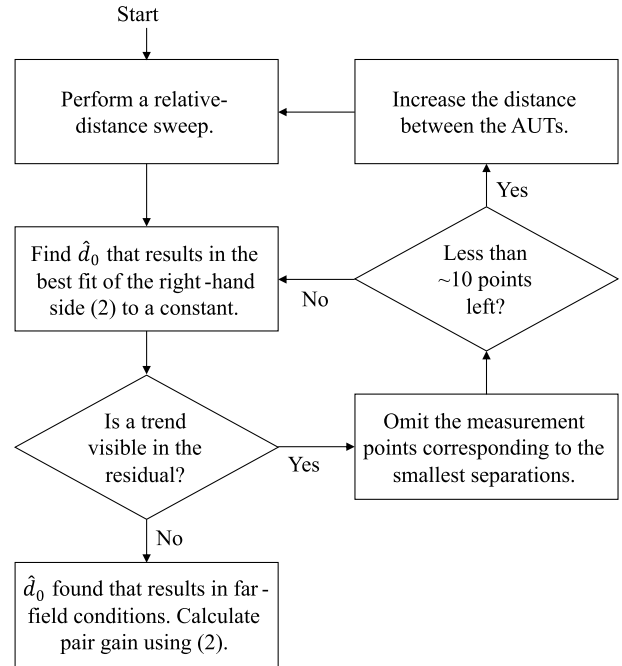


Fig. 7. Flowchart of the measurement technique to estimate \hat{d}_0 and the pair gain of one antenna pair.

Since no estimate of d_0 can be found that results in FF conditions, it can be concluded that the nonuniform phase distribution over the receiver's aperture is still significant for separations around 0.3 m. By iteratively reducing the data set and omitting the measurement points corresponding to the smallest separations, the regular pattern in the residual between the fit and a constant decreased and eventually disappeared. It was observed that from a separation of 0.8 m, FF conditions were met with a \hat{d}_0 of 23.7 mm as indicated in yellow in Fig. 6. It can be seen in the figure that the yellow line does not show a structural increase or decrease with respect to increasing Δd , indicating that both the nonuniform phase distribution is insignificant and that we found a suitable estimate for d_0 . In Fig. 7, a flowchart of the used approach is shown.

In Fig. 6, every solid line is accompanied by a converging black dashed line. These black lines are constructed using the model presented in Section IV-B. Also here, the black lines represent the determined realized pair gain of the antenna pair when the antennas are treated as point objects, for different errors in the estimation of the absolute distance between these point objects. The high degree of similarity from $\Delta d = 0.8$ m onward indicates that the solid lines corresponding to all three choices for \hat{d}_0 converge to the same pair gain of 42.4 dBi. However, since this value is already reached for $\Delta d = 0.8$ m and $\hat{d}_0 = 23.7$ mm, choosing $\hat{d}_0 = 23.7$ mm allows for gain measurements to be performed having FF conditions at a minimum antenna separation.

To determine the Fraunhofer distance, it is common to use the largest dimension of the largest AUT and is, therefore, independent of the other AUT. In both experiments described, the largest antenna was the same SGH, so for both the experiments, the Fraunhofer distance was 0.48 m. Note that in Fig. 4, it is shown that in the measurement with the OEWG and SGH, FF conditions are met above 0.3 m, whereas

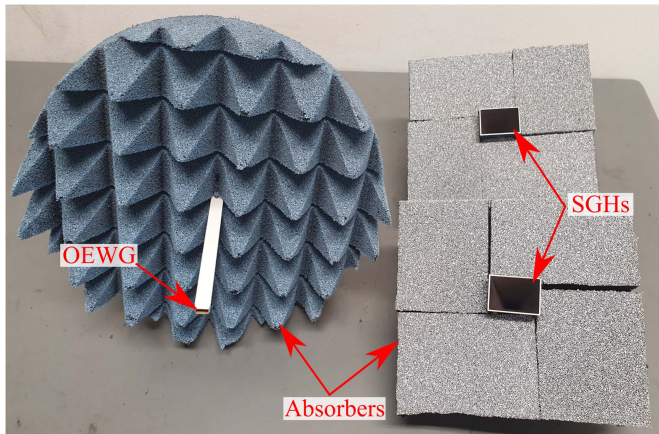


Fig. 8. Three K_a -band AUTs, including absorbing material to prevent reflections from the antenna mounts and flanges.

in Fig. 6, FF conditions are met above 0.8 m. This implies that although the Fraunhofer distance is usually considered to be independent of the smallest AUT, in practice, it depends on both AUTs from which distance FF conditions can be reached. This motivates the search for a new equation that can be used to calculate the minimum antenna separation required to achieve FF conditions. This is, however, beyond the scope of this article.

D. Determining the Realized Gain

The results in Figs. 4 and 6 show the realized pair gain of the AUTs. The goal of the gain measurement technique is eventually to determine the realized gain of an antenna. To determine the gain of an antenna using the three-antenna-method, first, the pair gain of each combination of three (unknown) antennas has to be determined. The three antennas that are used to acquire the data for this article are shown in Fig. 8. Two of the antennas are identical K_a -band SGHs from Flann Microwave⁴ (model 22240-20 [17]), and the other AUT is a K_a -band OEWG from NSI-MI Technologies (model ANT-WGP-26.5-40 [18]). Absorber material has been used to prevent reflections from the antenna mounts and flanges, as can be seen in Fig. 8. Since the two SGHs are nominally identical, the measurement results of each of the SGHs in combination with the OEWG shows very similar results. To prevent repetition of results, therefore, only the measurement results at 40 GHz for two of the three required distance sweeps are shown (see Figs. 4 and 6).

The true realized gain of the AUTs is not known. The gain values provided by the datasheet are based on a calculation and have a relatively large maximum possible error of ± 0.3 dB [19], making these values not a suitable reference. Instead, based on the dimensions provided in the datasheet, a 3-D model of the SGH was constructed to perform a full-wave simulation and is used as comparison. Since not all details of the antennas are available, and errors in manufacturing are not taken into account in the simulation models,

⁴The National Institute of Standards and Technology and Eindhoven University of Technology do not endorse commercial products. We use brand names only to better describe the experiments. Other products may work as well or better.

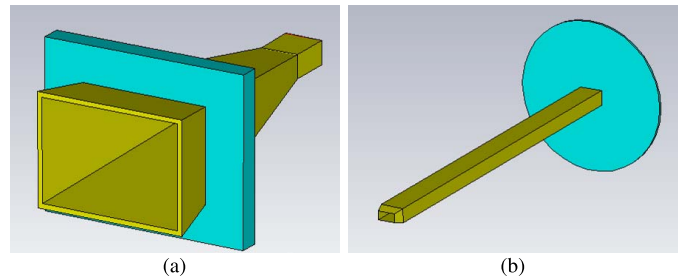


Fig. 9. CST models of (a) SGH and (b) OEWG.

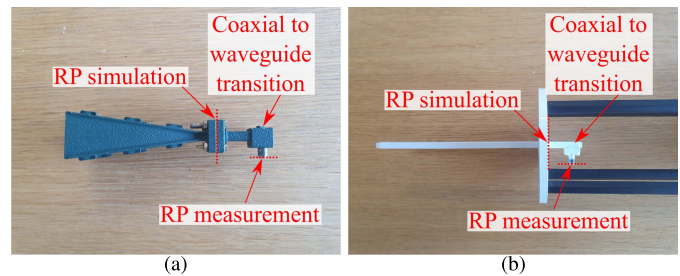


Fig. 10. Side view of (a) SGH and (b) OEWG, indicating the RPs in the measurement and in the simulation.

the simulation results are not treated as a reference, but as a check for the plausibility of the results obtained. The simulations were performed using CST Microwave Studio and the models are shown in Fig. 9. The metal conductors are made out of aluminum ($\rho = 3.56 \times 10^7$ S/m) and the absorbers are modeled by a surface impedance sheet having an impedance equal to the wave impedance of free space ($Z_{\text{abs}} = 377 \Omega$). Since the details of the 2.92 mm coaxial to WR28 waveguide transitions are not known, these adapters were not modeled, causing the RP of the simulation and measurement not to be at the same location, as can be seen in Fig. 10.

The simulated realized gain of the SGH is shown in Fig. 11 in purple. Moreover, the measured realized gain of both SGHs is shown in the figure as well. The difference in the measured gain of both SGHs is less than 0.02 dB on average and is maximum around 0.06 dB at the very end of the frequency band. Although the SGHs are identical, a deviation on the order of 0.02 dB on average is expected and can be attributed to manufacturing tolerances and uncertainties in the measurements. Moreover, the simulated and measured realized gain show the same trend, but there is still a reasonably large offset of about 0.2 dB on average present. As mentioned, the adapter is lacking in the simulation model. Therefore, a back-to-back measurement of the adapter was performed, and half the insertion loss of this measurement was subtracted from the simulation results in order to compensate for the adapter.⁵ The result is shown in Fig. 11, and we observed good agreement, strengthening the validity of the acquired results.

The measured realized gain of the OEWG is shown in Fig. 12 in blue. A peak-to-peak ripple on the order of 0.4 dB is visible on the realized gain. The reflection coefficient of the OEWG had been measured as well, and the ripple

⁵Strictly speaking, the full S -parameter matrix associated with this adapter has to be taken into account to compensate for the adapter. However, since the measured reflection coefficients of the back-to-back measurements were below -20 dB, the S_{11} and S_{22} of the adapter were assumed to be zero.

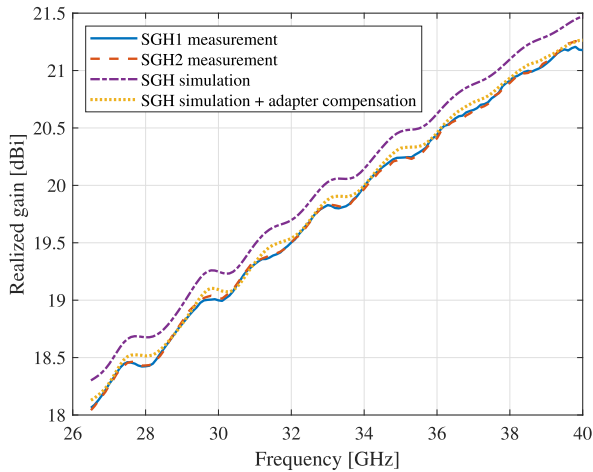


Fig. 11. Simulated and measured realized gain of the SGHs.

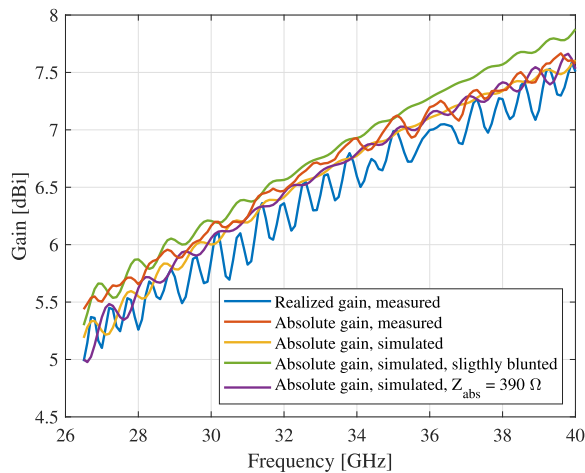


Fig. 12. Simulated and measured gains of the OEWG. Three simulated gains are depicted in order to show the sensitivity of the resulting gain with respect to small changes in the simulation setup.

on the realized gain was found to be present mainly due to the impedance mismatch of the OEWG. Since no information on the adapter is available and the OEWG consists of one metal piece making a back-to-back measurement of the adapter impossible, considering the absolute gain of the simulation and measurement of the OEWG results in a better comparison. In red and yellow, the measured and simulated absolute gains of the OEWG are shown. Still some discrepancies are present. This is mainly the result of the sensitivity of the gain to small changes in the simulation setup. For instance, in green, the simulated absolute gain is shown for the case where the edge of the tapered metal piece at the aperture is slightly blunted. As another example, in purple, the absolute gain is shown where the impedance of the absorbing material is changed to 390Ω . These slight changes in the simulation model show the sensitivity of the OEWG simulation model on the resulting gain, indicating that such a simulation is not suited for a detailed comparison. Despite this, the measured and the three simulated absolute gains show the same trend and are of the same order of magnitude, which shows that the acquired measured results are trustworthy.

In Fig. 13, the standard deviation of the uncertainty on the realized gain due to the fitting process is shown. As can be seen

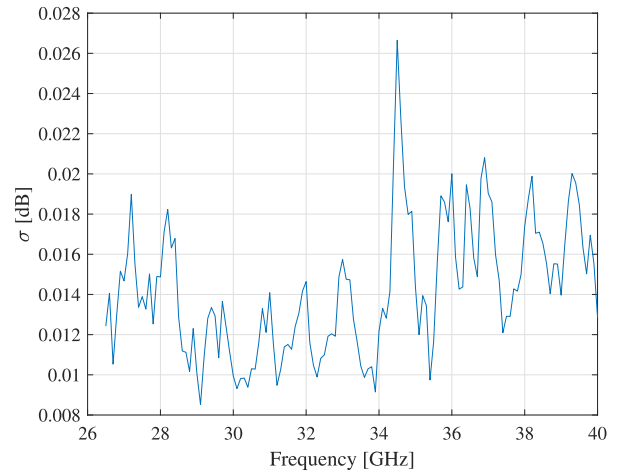


Fig. 13. Uncertainty of the fitted parameter (i.e., the realized gain).

in the figure, the uncertainty is less than 0.015 dB on average and has a maximum of 0.027 dB around 34.5 GHz. This uncertainty includes errors in the exact translation of the antenna, cable bending uncertainties, VNA drift, multipath scattering due to the nonideal anechoic environment, and reflections between both antennas. It does not include uncertainties in the values of the calibration standards and uncertainties in the alignment of the antennas. For some frequencies, especially around 34.5 GHz, the fitting uncertainty is dominated by the reflections between both antennas. Since these reflections are deterministic, they could be included in the model, resulting in a decreased fitting uncertainty. However, this results in additional complexity and is outside the scope of this article.

As mentioned, the true realized gain of the AUTs is not known. Therefore, the gains shown in this section cannot be validated. Due to uncertainties in the values of the calibration standards of the VNA and uncertainties in the alignment of the antennas, for instance, the true realized gain of the AUTs might very well be different from the realized gains reported in this section. However, the essence of the presented measurement technique is that we demonstrate a gain measurement method that ensures FF conditions. It should, therefore, be emphasized that although the reported realized gains cannot be validated, the compliance with the definition of the realized pair gain (and thus realized gain) being constant with respect to separation, as shown in Figs. 4 and 6, does validate that FF conditions are met. This, in turn, validates the measurement technique we present here.

V. EVALUATION OF THE GAIN MEASUREMENT TECHNIQUE

A. Comparison to Different Choices of Reference Points

The curves in Figs. 4 and 6 showed the impact of the choice of reference point on the determined realized pair gain for one frequency. In Fig. 14, the difference in the realized gain over the entire K_a -band for different choices of reference points is shown, for three separations. The gain of the SGHs shown in Fig. 11 is treated as the reference. In Fig. 14, the reference points of the antennas are once again chosen to be at the aperture (blue), at one-third of the SGH's flare length (red) and determined for each frequency by the fitting routine (yellow).

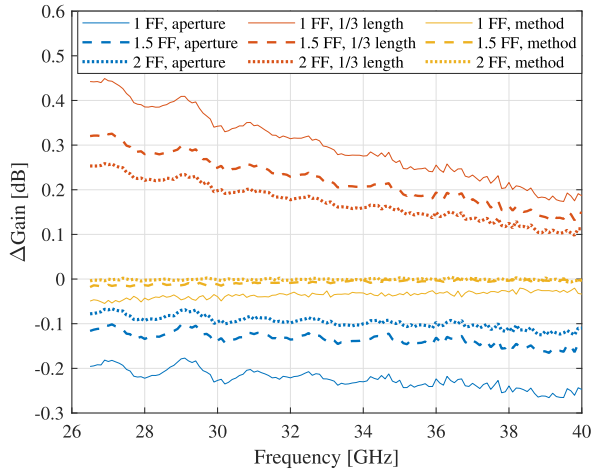


Fig. 14. Improvement of the gain estimation of one of the SGHs by the presented gain measurement technique over choosing the reference point at the aperture (blue) or at one-third of the flare length (red) for different separations. The solid, dashed, and dotted lines represent a separation (measured from aperture to aperture) of 1, 1.5, and 2 times the Fraunhofer FF distance, respectively.

The solid, dashed, and dotted lines represent a separation of 1, 1.5, and 2 times the Fraunhofer FF distance, respectively. This separation is measured from aperture to aperture. As expected, for increased separation, the differences go toward zero. However, as can be seen in the figure, for a separation as small as the Fraunhofer distance, the error in gain can be on the order of 0.2 dB or higher if the choice of reference point is poor. This emphasizes the importance of determining a good reference point for limited antenna separations and strengthens the usability of the presented method.

Note that the error contribution in the gain estimation shown in Fig. 14 is independent of uncertainties in the calibration standards or mechanical alignment. Hence, the figure solely shows the induced error by having a poor choice of reference point.

B. Comparison Phase and Amplitude Center

For each of the three combinations of antennas, a value for d_0 is determined for each frequency. For $\Delta d = 0$, the apertures were connected to each other, which means that in the presented measurements, d_0 represents the sum of the amplitude centers of both antennas with respect to their apertures. Similar to how the gain of the individual antennas can be determined by manipulating the three determined pair gains, the amplitude center of the individual antennas can be extracted by manipulating the three sums of amplitude centers. In Fig. 15, the amplitude center of the two assessed SGHs is shown in blue and red. Note that the distance being positive means that the amplitude center is inside the SGH.

In Section II, a short discussion on the difference between the amplitude center and phase center is given. Since both concepts describe a point where radiation seemingly originates from, the question might arise as to whether the same antenna gains as shown in Figs. 11 and 12 could have been acquired if a simulated or measured phase center was used. Since the position of the phase center of an antenna is not uniquely defined as it depends on “the portion of the surface of the

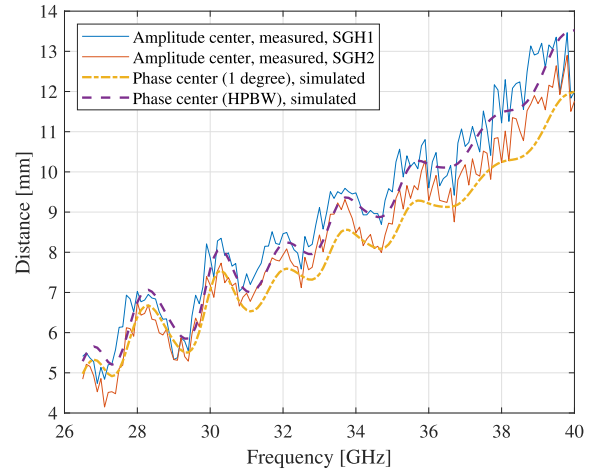


Fig. 15. Measured amplitude centers and simulated phase centers of the SGHs.

radiation sphere where radiation is significant,” we evaluated two extremes. Typically, the region corresponding to the half-power beamwidth (HPBW) of the antenna is regarded as the significant region [6]. The HPBW was minimally 15° in both the E- and H-plane over the entire frequency band, so an angular region of $\pm 7.5^\circ$ is used to determine the phase center. On the other hand, the minimum angular region that can be used to determine the phase center in CST is $\pm 1^\circ$, so the calculated phase center using that angular region is evaluated as well. In Fig. 15, the phase centers of the SGH as determined by a built-in function of CST are also shown. Although the phase center is not uniquely defined, both simulated phase center curves show a very similar trend to the amplitude centers of the SGHs. This implies that taking the distance between the antennas based on a simulated phase center, the realized gain would not differ significantly from the realized gain shown in Fig. 11.

The measured amplitude center and simulated phase centers of the OEWG are shown in Fig. 16. It can be clearly seen that the two different choices of angular region that were assessed give rise to two completely different phase center locations as a function of frequency. At some frequencies, the difference is on the order of a wavelength. Additionally, the measured amplitude center shows totally different behavior. As can be seen in the figure, the absolute distance between the antennas can be off by a wavelength if this distance is based on a simulated phase center. In turn, this can result in an error of 0.2 dB in the determined gain of the AUTs for a separation on the order of the Fraunhofer distance. This emphasizes the importance of using the amplitude center and not the phase center (regardless of the angular region used to determine this location) as the antenna’s reference point.

C. Number of Measurements in the Distance Sweep

Although from a separation of 0.3 and 0.8 m onward, the fitted data (yellow) in Figs. 4 and 6, respectively, do not show an increasing or decreasing trend, still the fitted data are not completely flat. This is most likely due to scattering from the environment, reflections from the opposite antenna, and uncertainties in the exact displacement of the translated

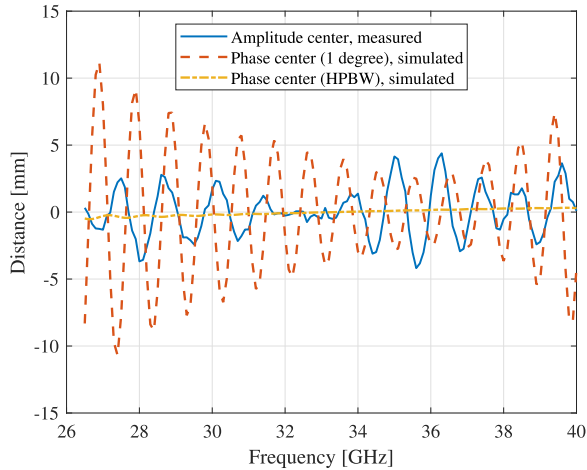


Fig. 16. Measured amplitude center and simulated phase centers of the OEWG.

antenna. An advantage of the presented measurement method is that since multiple measurements are taken, the impact of these effects is averaged. For this work, the transfer between the AUTs has been measured for hundreds of different separations to properly show the principle of the presented measurement technique. For practical purposes, it would be convenient if accurate results could be obtained with far fewer measurements.

In theory, only two measurements are required to determine the two unknowns which are present in (2). A third measurement is required to assess whether FF conditions are met, thus verifying that the nonuniform phase distribution is insignificant. Due to nonideal measurement conditions, as, for instance, scattering, more measurement points are recommended. It is impractical to define, in general, how many measurements are required in order to achieve a certain accuracy, as this mainly depends on the measurement setup. However, based on the data acquired for this article, some guidelines can be drafted.

The following results are based on the data presented in Fig. 6. It is shown in Fig. 6 that FF conditions were met from 0.8 m onward. However, it is, in general, not known how large the antenna separation must be before FF conditions are met. In Fig. 17, the pair gain determined by the fitting routine is shown for different truncated data sets. As a first step, the data set is truncated representing a measurement from 0.5 to 1.3 m with a step size of 10 mm (81 points). The fitting routine is used to estimate d_0 , and the determined pair gain for each of the individual measurement points is illustrated in Fig. 17 using the blue circles, with an average indicated by the blue dotted line. By looking at the difference between the individual measurement points and the average determined pair gain, a regular pattern in the residual can be observed. To illustrate this, a quadratic fit to this data set has been added in Fig. 17, depicted by the blue dashed line. This regular pattern in the residual indicates that FF conditions are not met for this data set. Therefore, the data set is truncated further, from 0.8 to 1.3 m, having a step size of 10 mm (51 points). The result is shown using the red crosses. No clear recognizable pattern in the residual is present, indicating that FF conditions are met for this data set.

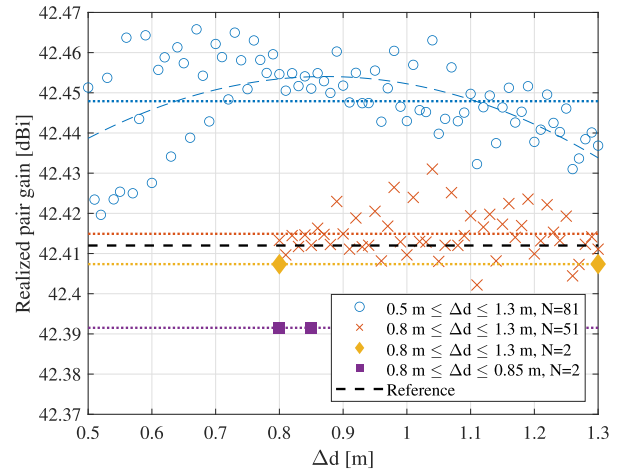


Fig. 17. Comparison of the gain for different truncated data sets.

As a next step, the data set is reduced to two points, and the results are shown using yellow diamonds (0.5 m separation) and purple squares (50 mm separation). The pair gain is, even for two measurement points, very close to the pair gain determined by the full data set, which is illustrated by the black dashed line and denoted by “Reference.” This implies that when FF conditions are met, and no significant scatterers are present, having two measurement points can provide sufficient accuracy. However, with only two points, it is not possible to verify whether FF conditions are met because the residual between the fit and individual measurement points will always be zero, as can be seen in Fig. 17. Therefore, taking more than two measurements is recommended.

D. Reduced Error Versus Increased Costs and Complexity

An automatically controlled translation stage was used to acquire the measurement data for this article. Embedding a translation stage in an (existing) anechoic chamber can be expensive. As antenna gain measurement uncertainties are sometimes dominated by uncertainties in the mechanical alignment of the antennas, especially if highly directional antennas are used, implementing the proposed method can be economically unattractive. However, if high-quality measurements are required to reduce risk of failure, as is often the case in space applications, these types of investments could be attractive. Moreover, small millimeter-wave anechoic chambers are currently under development [15], [16] and including a translation stage in these chambers can very well be cost effective. In the end, it is up to the reader whether or not the reduced error in gain determination outweighs the increased costs and complexity associated with the proposed technique.

E. Connection to the Extrapolation Measurement Technique

In this article, the Friis equation is used to model the interaction between two antennas. Wacker’s equation offers a more rigorous description than the Friis equation and is used in the extrapolation measurement technique [1], [14]. When using this measurement technique, a similar relative-distance sweep as used in the presented method is performed. Subsequently, the data is fitted to a polynomial that accounts for

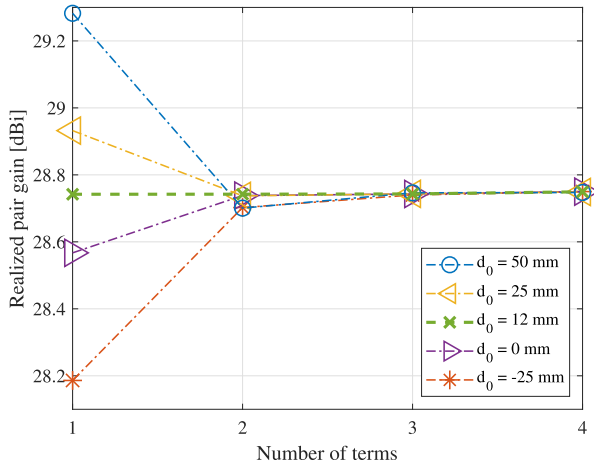


Fig. 18. Comparison of the pair gain determined from (5) for different number of terms and for different values of d_0 .

the phase curvature over the receiver's aperture and standing waves between the antennas. Moreover, as claimed in [14], the pair gain determined using the extrapolation method is independent of the choice of reference point. Although this is true, it might not be immediately clear how the choice of reference point affects the fit of the extrapolation method.

To conceptually show the connection of the extrapolation method to the presented method, we fit the polynomial in Wacker's equation that describes the zeroth order of scattering to the data acquired in the measurement using the OEWG and SGH (see Section IV-A) at 40 GHz from $\Delta d = 0.3$ m to $\Delta d = 1$ m for different choices of d_0 . The absolute value of the zeroth order of scattering can be written as follows:

$$|S_{21}| = \frac{\lambda_0}{4\pi d} \sum_{n=0}^{\infty} \frac{A_n}{d^n} = \frac{\lambda_0}{4\pi d} \left(A_0 + \frac{A_1}{d} + \frac{A_2}{d^2} + \dots \right) \quad (5)$$

with A_n the constants that are to be determined by a least-squares fit. The constant A_0 represents the square root of the pair gain. Hence, determining A_0 is the objective when using the extrapolation method. If the distance d is large, only the first term of the polynomial is significant such that we arrive at the Friis equation. Note that $d = \Delta d + d_0$, so the constants A_n in (5) are implicitly a function of d_0 .

Equation (5) contains infinitely many terms. Thus, selecting the optimum number of terms is not always a trivial task. In Fig. 18, the pair gain for different number of terms and for different values of d_0 is shown. It can be seen in the figure that if the model only consists of one term, all choices of d_0 result in a different pair gain. If a three-term or four-term model is selected, all five choices of d_0 result to the same pair gain, verifying the claim the pair gain determined using the extrapolation method is independent of d_0 . The pair gain for a d_0 of 12 mm is independent of the number of terms, implying that a one-term model is suitable for $d_0 = 12$ mm. Hence, the number of terms required to fit the data accurately can be reduced by making a good estimate of d_0 , reducing the risk of overfitting, in turn.

In this example, only data that complied with the inverse-square law are considered and higher order scattering terms were omitted. To thoroughly show the impact of choosing a reference point on the ability to fit Wacker's equation to the

data and avoid the risk of overfitting, those effects have been taken into account as well. This is, however, beyond the scope of this article.

VI. CONCLUSION

In this article, a gain measurement technique based on a relative-distance sweep is presented. Using this measurement technique, the distance between amplitude centers of the antennas can be found. Knowing the absolute distance between the antennas allows for accurate gain measurements to be performed at limited separations. Moreover, performing measurements at multiple different distances allows the impact of the nonuniform phase curvature over the receiver's aperture on the determined gain to be assessed, and thus whether or not the distance between the antennas has to be increased in order to achieve FF conditions. Furthermore, since multiple measurements are taken, scattering and errors in the exact displacement of the translated antenna are averaged, hence, reducing the error in the determined gain. These properties make the presented gain measurement technique suitable for accurate gain determination (having a fitting uncertainty on the order of hundredths of dBs) in small anechoic chambers where the separation between the antennas is limited, that is, on the order of one or two times the Fraunhofer FF distance.

REFERENCES

- [1] A. Newell, R. Baird, and P. Wacker, "Accurate measurement of antenna gain and polarization at reduced distances by an extrapolation technique," *IEEE Trans. Antennas Propag.*, vol. AP-21, no. 4, pp. 418–431, Jul. 1973.
- [2] H. T. Friis, "A note on a simple transmission formula," *Proc. IRE*, vol. 34, no. 5, pp. 254–256, May 1946.
- [3] *IEEE Standard Test Procedures for Antennas*, Standard ANSI/IEEE Std 149-1979, 1979, pp. 78–98.
- [4] K. T. Selvan and R. Janaswamy, "Fraunhofer and Fresnel distances: Unified derivation for aperture antennas," *IEEE Antennas Propag. Mag.*, vol. 59, no. 4, pp. 12–15, Aug. 2017.
- [5] R. R. Bowman, "Field strength above 1 GHz: Measurement procedures for standard antennas," *Proc. IEEE*, vol. 55, no. 6, pp. 981–990, Jun. 1967.
- [6] S. Pivnenko, J. M. Nielsen, and O. Breinbjerg, "Using the phase center of a standard gain horn in antenna gain determination," in *Proc. Antenna Meas. Techn. Assoc. Symp. (AMTA)*, Boston, MA, USA, 2008, pp. 334–340.
- [7] S. Pivnenko and O. Breinbjerg, "Fast and accurate measurement of on-axis gain and on-axis polarization at a finite distance," in *Proc. 7th Eur. Conf. Antennas Propag. (EuCAP)*, Gothenburg, Sweden, 2013, pp. 810–814.
- [8] K. Harima, M. Sakasai, and K. Fujii, "Determination of gain for pyramidal-horn antenna on basis of phase center location," in *Proc. IEEE Int. Symp. Electromagn. Compat.*, Detroit, MI, USA, Aug. 2008, pp. 1–5.
- [9] K. Harima, "Accurate gain measurement for millimeter-wave horn and open-ended waveguide antennas," in *Proc. Int. Symp. Antennas Propag. (ISAP)*, Nagoya, Japan, 2012, pp. 1019–1022.
- [10] K. Harima, "Evaluating the effectiveness of applying the phase center for antenna measurements," in *Proc. IEEE Conf. Antenna Meas. Appl. (CAMA)*, Tsukuba, Japan, Dec. 2017, pp. 61–64.
- [11] T. W. Hertel, "Phase center measurements based on the three-antenna method," in *Proc. IEEE Antennas Propag. Soc. Int. Symp. Held Conjoint*, Columbus, OH, USA, Jun. 2003, pp. 816–819.
- [12] *IEEE Standard for Definitions of Terms for Antennas*, Standard IEEE Std 145-2013 Revision of IEEE Std 145-1993, Mar. 2014, p. 25.
- [13] J. Appel-Hansen, "Centers of structures in electromagnetism—a critical analysis," *IEEE Trans. Antennas Propag.*, vol. AP-30, no. 4, pp. 606–610, Jul. 1982.
- [14] A. J. Yuffa, "On Wacker's essential equation in the extrapolation measurement technique," in *Proc. Antenna Meas. Techn. Assoc. Symp. (AMTA)*, San Diego, CA, USA, Oct. 2019, pp. 1–5.

- [15] A. B. Smolders, A. C. F. Reniers, U. Johannsen, and M. H. A. J. Herben, "Measurement and calibration challenges of microwave and millimeter-wave phased-arrays," in *Proc. Int. Workshop Antenna Technol. (iWAT)*, Karlsruhe, Germany, Mar. 2013, pp. 358–361.
- [16] R. Schwarz. (Jun. 2020). *R&S ATS1000—Brochures and Data Sheets*. [Online]. Available: <https://www.rohde-schwarz.com/fi/brochure-datasheet/ats1000/>
- [17] Flann Microwave. (Jun. 2020). *Standard Gain Horns Series 240*. [Online]. Available: <https://flann.com/products/antennas/standard-gain-horns-series-240/>
- [18] NSI-MI. (Jun. 2020). *Waveguide Probes*. [Online]. Available: <https://www.nsi-mi.com/products/antenna-products/waveguide-probes/>
- [19] W. T. Slayton, "Design and calibration of microwave antenna gain Standards," US Nav. Res. Lab., Washington DC, USA, Tech. Rep. 4433, 1954.



A. J. (Teun) van den Biggelaar received the M.Sc. degree (Hons.) in electrical engineering (EE) from the Eindhoven University of Technology (TU/e), Eindhoven, the Netherlands, in 2016, and the Ph.D. degree (Hons.) from the Electromagnetics (EM) Group, Department of EE, TU/e, in 2020. His M.Sc. thesis was selected as the best M.Sc. thesis of the Department of EE in the year 2016.

During his Ph.D., he worked on a project supported by NXP Semiconductors, Nijmegen, the Netherlands. Additionally, he had been a Guest Researcher at the National Institute of Standards and Technology (NIST), Boulder, CO, USA, for a period of six months. Currently, he is a Guest Researcher at TU/e and focuses on over-the-air measurement systems and techniques for millimeter-wave 5G antenna systems.



S. J. (Sander) Geluk received the B.Sc. and M.Sc. degrees (Hons.) in electrical engineering (EE) from the Eindhoven University of Technology (TU/e), Eindhoven, the Netherlands, in 2012 and 2015, respectively, and the Ph.D. degree (Hons.) from the Electromagnetics (EM) Group, Department of EE, TU/e, in 2019.



B. F. (Benjamin) Jamroz received the Ph.D. degree in applied mathematics from the University of Colorado, Boulder, CO, USA, in 2009, where he developed new analytical and numerical models for plasma physics.

As a Computational Scientist, his work includes modeling physical phenomena, including electromagnetics and fluid dynamics as well as applying machine learning techniques. In 2017, he joined the Communications Technology Laboratory, National Institute of Standards and Technology, where he models and analyzes the complex systems required for high-frequency communications.



D. F. (Dylan) Williams (Life Fellow, IEEE) received the Ph.D. degree in electrical engineering from the University of California at Berkeley, Berkeley, CA, USA, in 1986.

He joined the Electromagnetic Fields Division, National Institute of Standards and Technology, Gaithersburg, MD, USA, in 1989, where he develops electrical waveform and microwave metrology. He has published over 100 technical papers.

Dr. Williams was a recipient of the Department of Commerce Bronze and Silver Medals, the Astin Measurement Science Award, two Electrical Engineering Laboratory's Outstanding Paper Awards, three Automatic RF Techniques Group (ARFTG) Best Paper Awards, the ARFTG Automated Measurements Technology Award, the IEEE Morris E. Leeds Award, the European Microwave Prize, and the 2013 IEEE Joseph F. Keithley Award. He also served as an Editor for the IEEE TRANSACTIONS ON MICROWAVE THEORY AND TECHNIQUES from 2006 to 2010, the Executive Editor for the IEEE TRANSACTIONS ON TERAHERTZ SCIENCE AND TECHNOLOGY, and as the 2017 President of the IEEE Microwave Theory and Techniques Society.



A. B. (Bart) Smolders (Senior Member, IEEE) is the Dean of the Department of Electrical Engineering, Eindhoven University of Technology (TU/e), Eindhoven, the Netherlands. Next to this, he is a Full Professor and the Chair of the Electromagnetics (EM) Group. His key areas of expertise include telecommunication engineering, antenna systems, and microwave engineering. In the EM Research Group, his main focus is advanced integrated antenna systems and related applications, such as phased arrays and focal-plane arrays for future wireless communications. His team is collaborating on a number of European and national projects, including SILIKA (Silicon-based *Ka*-band massive MIMO antenna systems for new telecommunication services), EAST (tunable antenna concepts for 5G mobile), Integrant (90 GHz wireless point-to-point systems), MUSIC (60 GHz single-chip MIMO radar), and SMART-One (millimeter-wave channel sounding).



U. (Ulf) Johannsen (Member, IEEE) received the Dipl.-Ing. degree in communications engineering from the Hamburg University of Technology (TUHH), Hamburg, Germany, in 2009, and the Ph.D. degree in electrical engineering from the Eindhoven University of Technology (TU/e), Eindhoven, the Netherlands, in 2013.

He then started as a Senior Systems Engineer at ATLAS ELEKTRONIK GmbH, Bremen, Germany, where he worked as a System Designer and an Engineering Manager on autonomous underwater vehicle (AUV) systems with sonar payloads. In 2016, he was appointed an Assistant Professor with the Electromagnetics Group, TU/e Department of Electrical Engineering.

Dr. Johannsen is the Chair Person of the IEEE Benelux joint AP/MTT chapter.



L. A. (Sander) Bronckers (Member, IEEE) received the M.Sc. degree (*cum laude*) in electrical engineering from the Eindhoven University of Technology (TU/e), Eindhoven, the Netherlands, in 2015, and the Ph.D. degree (*cum laude*) in electrical engineering from the Electromagnetics Group, TU/e, in 2019, with a focus on design and measurement techniques for next-generation integrated antennas.

In 2018, he was a Visiting Researcher at NIST, Boulder, CO, USA, on antenna measurements in reverberation chambers. He is currently an Assistant Professor on metrology for antennas and wireless systems at TU/e. His research interests include antenna measurements in reverberation and anechoic chambers, channel sounding and emulation, and RF material characterization.